Registration between respiratory-gated PET/CT and high-resolution CT with XCAT simulations: evaluation and optimization for subsequent PVC

A. Turco[1], J. Nuyts[1], O. Gheysens[1], J.U. Voigt[2], P. Claus[2], K. Vunckx[1]

***Abstract*—Registration of a high-resolution CT (HRCT) to a low-resolution PET has been shown to enable enhanced PET image quality. The CT can be used as prior information for partial volume correction (PVC) during reconstruction, provided that it is accurately registered to the PET dataset of interest.**
By means of simulations using an XCAT phantom, this work analyzes the impact of different attenuation correction protocols on HRCT to PET registration. The focus of this work is on cardiac images with only respiratory motion taken into account, with the aim of optimally aligning the left-ventricular region in PET and HRCT. Shallow breathing was simulated and so far only noise-less data were evaluated. Also, a comparison to registration results from a deep breathing phantom has been performed.
As expected, results speak in favour of using an ideal, perfectly matching attenuation correction map (ACM). However, when using an average or a single respiratory phase ACM accurate alignment can still be achieved. Registration of non-attenuation-corrected images requires further investigation, as it seems to be strongly dependent on the initial alignment of PET and CT.

I. Introduction

The measurement of ^{18}F-Fluorodeoxyglucose (FDG) uptake by positron emission tomography (PET) is a validated and robust tool to investigate myocardial glucose metabolism [1]. FDG PET can provide useful parameters and standard indicators of the workload of the heart [2], which in turn could be related to the health status of the organ itself. Limitations of the current PET imaging instrumentation make yielding images with satisfactory diagnostic quality difficult. The relatively low spatial resolution (5-6 mm) of PET does not allow for distinguishing between thinned healthy cardiac walls and normal walls with reduced metabolism. This partial volume effect (PVE) hampers making correct diagnoses [3].
In addition, extracting valuable and correct information from cardiac images is not straightforward due to the moving nature of the heart. Being located in the thoracic cavity, the heart is subject to respiratory motion, whose contribution has to be added to the artefacts introduced by the heartbeat. Various techniques have been developed to overcome, at least partially, the aforementioned challenges [4]–[8]. One of the most common and straightforward solutions, though not optimal for image quality, is to sort the PET dataset into a set of frames corresponding to the different phases of the periodic motion, and then independently reconstruct and use each frame (i.e. gating). After gating, partial volume correction (PVC) during PET reconstruction may be applied using a CT image with high spatial and temporal resolution (coming from a dedicated CT scanner), in order to improve PET image quality [9]. To this end, the high-resolution CT and the low-resolution PET need to be perfectly aligned, hence any source of misalignment needs to be avoided.

In this scenario, PET attenuation correction might play a role in compromising the registration results.
Almost every contemporary PET scanner incorporates a CT scanner, which a.o. is used to acquire low-dose, low-resolution CT images from which an attenuation correction map (ACM) of the various tissues can be estimated, and appropriate corrections to the PET data can be applied. Some studies encourage the use of an average CT to reduce the artefacts, while other groups correct the PET data with a fast CT where breathing motion is frozen into a single phase [10]. As both approaches are expected to introduce errors during the attenuation correction process, it is also interesting to see what would happen to the registration accuracy if no attenuation correction is applied to the PET images.
In cardiac PET imaging, PET attenuation correction performed with an average, low-dose CT has been shown to produce no significant artefacts when only shallow respiratory motion is involved [11]. However, to our knowledge, nothing has been said so far on the influence of the use of an average attenuation correction map on the quality of PET to high-resolution CT registration, both in the case of shallow and deep breathing. Moreover, the effect of using other attenuation correction protocols has never been tested.

The aim of this work is to assess the influence of attenuation correction on the quality of image registration between respiratory-gated cardiac PET images and high-resolution CT images, when only respiratory motion is taken into account. Attention is focused on the accurate alignment of the left-ventricles in PET and HRCT.
The effect of different attenuation correction strategies is investigated, with particular attention to the results obtained when cropping the PET and the CT images to the heart

[1] Medical Imaging Research Center, Dept. of Nuclear Medicine, University Hospitals Leuven & Dept. of Imaging & Pathology, KU Leuven, B-3000 Leuven, Belgium. [2] Medical Imaging Research Center, Dept. of Cardiology, University Hospitals Leuven & Dept. of Cardiovascular Sciences, KU Leuven, B-3000 Leuven, Belgium.

This work is supported by KU Leuven OT/12/084 and Research Foundation - Flanders

region before registration. The datasets used for this purpose are obtained by means of simulations, using a realistic digital anthropomorphic phantom, the XCAT [12].

The rest of this paper is organized as follows:
In section II, the details of the phantom used are given, together with a description of the registration and evaluation methods. In section III, an overview of the results is presented, with particular emphasis on the cropped images. In addition, a comparison between the shallow and deep breathing scenario is shown.
Conclusions and future directions are provided in section IV.

II. Methods

In this work, the XCAT software [12] has been used to generate a PET dataset with 8 respiratory gates, an image corresponding to a HRCT and 3 different ACM sets. Details on the phantom generation are given in section II-A. These ACMs were used during PET image reconstruction (see section II-B), resulting in the following sets of PET reconstructed images:

- **'PERFCT'**: a different ACM was used to correct each PET gate. In this ideal case, the attenuation map perfectly matches the PET respiratory phase, thus leading to optimal, artefact-free PET reconstructions. Note that these ACMs were also used during PET sinogram generation.
- **'AVCT'**: an ACM obtained by averaging all ACMs over a breathing cycle was used to correct all individual PET gates.
- **'SPHCT'**: the ACM corresponding to a single phase of the respiratory cycle was used to correct for attenuation in all PET gates.
- **'NOATTEN'**: the last dataset consisted of PET images reconstructed without any attenuation correction.

Each of these datasets was then registered to the HRCT (see section II-C), and evaluation of the registration results was performed as explained in section II-D.
Figure 1 provides an overview of the full workflow.

The rest of this section elaborates each of the above mentioned steps.

A. Phantom generation

4D PET images of the thoracic region were simulated using the XCAT phantom. Three phantoms were generated in order to produce the PET dataset, the various attenuation correction maps and the HRCT. They will be referred to as *PET phantom*, *HRCT phantom* and *SPHCT phantom*.

The *PET phantom* was an average male phantom, with arms up as proposed in [13], used to obtain the PET dataset, the average and the perfect ACMs.

Realistic, homogeneous FDG uptake values were assigned to the different organs and tissues of the simulated phantom. Beating motion was not taken into account and only respiratory motion was simulated. The respiratory cycle was divided into 8 equally spaced time frames (gates), for a total cycle duration of 4.3 s. From one frame to the next, the heart

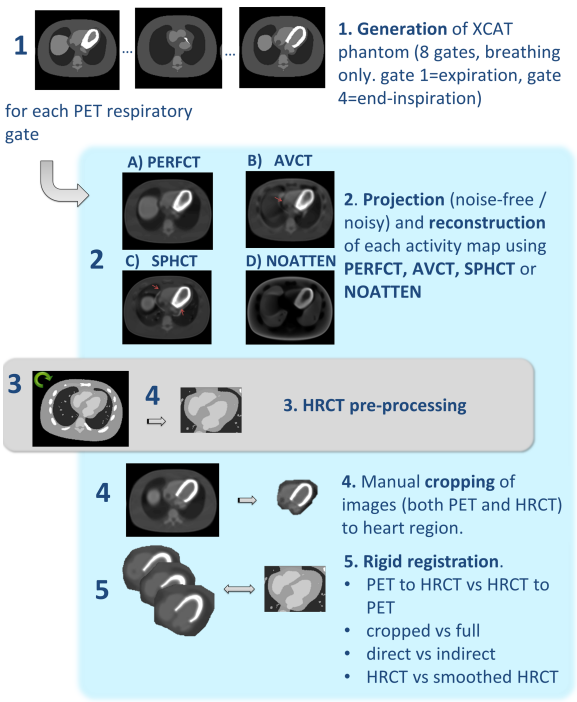

Fig. 1. Work flowchart, illustrated for quiet breathing.

motion is solely due to the effect of respiration. Both deep and shallow breathing were simulated. In both cases, realistic motion parameters were used [14] [15]. An overview of the main parameters used to generate the *PET phantom* is on Table I.

TABLE I. Key parameters for phantom generation.

	Shallow breathing	Deep breathing
Antero-posterior (AP) expansion [cm]	0.3	1.8
Diaphragm motion [cm]	1.54	6.20
Resp. cycle[s]	4.3	4.3
No. gates/cycle	8	8
Phantom size [pixel]	750x750x203	750x750x203
Phantom pixel size [mm]	0.8	0.8

Eight corresponding attenuation maps and an average attenuation map were also generated with the same parameters.

The *SPHCT phantom* was generated to obtain the SPHCT ACM. The *SPHCT phantom* is everywhere identical to the *PET phantom*, except for the respiratory start phase index which was set to 6%. The 6th attenuation correction map belonging to the resulting *SPHCT phantom* was used as the single phase attenuation correction map (SPHCT).

Finally, the *HRCT phantom* was generated to obtain a high-resolution CT image in a posture and a breathing phase that was slightly different from that in the PET/CT system. For that purpose, the *HRCT phantom* was generated with the following parameters different from the *PET phantom*:

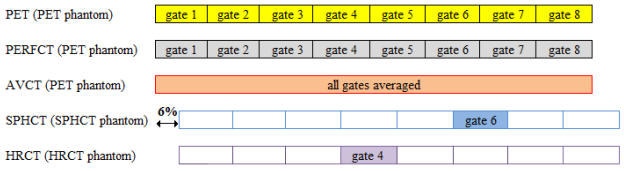

Fig. 2. Phantoms generated with the XCAT software.

- AP expansion: 0.7 cm (quiet breathing) and 1.5 cm (deep breathing).
- Maximum extent of diaphragm motion: 2 cm (shallow breathing) and 5 cm (deep breathing).
- Respiratory start phase index: 6% phase shift (0% = full exhale, 40% = full inhale), to simulate a slight respiratory mismatch between corresponding *PET* and *HRCT phantom* gates (see Fig. 2).

The 4th simulated attenuation map belonging to the *HRCT phantom*, corresponding to end-inspiration phase, was converted to Hounsfield units and a small rotation and translation were applied to it, to simulate patient positioning differences between the PET/CT scan and HRCT scan. Three different initial roto-translations were applied to the HRCT ("parms 0", "parms 2", "parms 18"), to better see the effect of those pose differences on the registration results.
The generated HRCT images served as the target high-resolution CTs, to which all PET frames should be registered.

Figure 2 gives a visual overview of the generated phantoms.

All attenuation and activity maps were created using a voxel size of $(0.8mm)^3$.

B. Projection and reconstruction of XCAT phantom

Eight noise-free PET sinograms were generated by projecting each of the 8 activity distribution images from the *PET phantom* using in-house software that simulates the behaviour of the Siemens Biograph 16 PET/CT (HIREZ) scanner [16]. Attenuation and spatially invariant camera resolution (gaussian kernel with full width at half-maximum (FWHM) of 4.3 mm) were modelled, but scatter and randoms were not.

Each gated sinogram was reconstructed using a 3D ordered subsets-expectation maximization (OSEM) algorithm with resolution modeling (4 iterations and 16 subsets per iteration). As mentioned earlier, four different attenuation correction strategies were applied during reconstruction, resulting in the 4 different PET datasets (PERFCT, AVCT, SPHCT, NOATTEN). Cubic reconstruction voxels of 2 mm were used. The same AC procedures were applied to the noisy sinograms.

All reconstructed PET datasets were cropped to the heart region. The shape of cropping was arbitrary as long as it contained the whole heart, both axially and transaxially. Same gates (of the same breathing pattern) received the same cropping, in order not to influence registration results with an additional possible source of misregistration. The HRCT images were also cropped, using a rectangular box and similar considerations apply.

C. Registration

Rigid registration was performed in this work, based on the fact that no beating motion was modeled and respiratory motion mainly causes the heart to translate in the cranio-caudal direction, and to a lower extent in the antero-posterior direction [17]. Rigid registration was performed using both cropped and full images, being aware that the registration between full images can only be effective in the somewhat unlikely case that the heart movement determines the main variations of the mutual information of the images over a breathing cycle. Normalized mutual information (NMI) was chosen as the matching criterion, since it has been proved particularly effective for inter-modality image registration [18], especially if partially overlapping images are involved. In order to possibly take advantage of faster registration times, we tested both the registration of the low-resolution PET to the HRCT (PET-to-HRCT) and vice versa (HRCT-to-PET).

Moreover, to further decrease the influence of non–cardiac voxels on the registration, the effect of an additional, simple masking applied to the HRCT was investigated. All the pixels with a Hounsfield value smaller or equal to zero were ignored in the construction of the joint histogram, which later serves for the calculation of the NMI cost function. Basically, this removes the contribution of the lungs and fat to the joint histogram.

Extremely poor registration results can be expected when the respiratory phases to be matched are very different (e.g. end-expiration PET to end-inspiration HRCT, especially when deep-breathing motion is modeled) or when the initial misalignment between PET and HRCT is not negligible compared to the movement of the heart. In those cases, a preliminary image alignment was performed. This step implied a preliminary registration of the n-th PET gate to the PET gate that best corresponded to the HRCT (i.e. PET gate 4) using normalized cross correlation. Only afterwards, the n-th PET gate image was registered to the HRCT, starting from the resulting, better initialized transformation parameters.

In addition, it was evaluated whether decreasing the resolution of the HRCT to the level of the PET improved the registration accuracy. To this end, a smoothed replica of each HRCT was generated with a spatially-invariant Gaussian kernel with FWHM = 4.3 mm.

D. Evaluation of results

Evaluation of PET-to-HRCT and HRCT-to-PET registrations was performed in PET space, as this will be the space where PVC is applied. The registered images were evaluated first by visual inspection. In addition, DICE-Sørensen coefficients (DSC) were calculated to quantify the overlap between the left ventricular (LV) regions. For this purpose, in the case of PET-to-HRCT registration, the inverse transformation parameters were applied to the CT image.

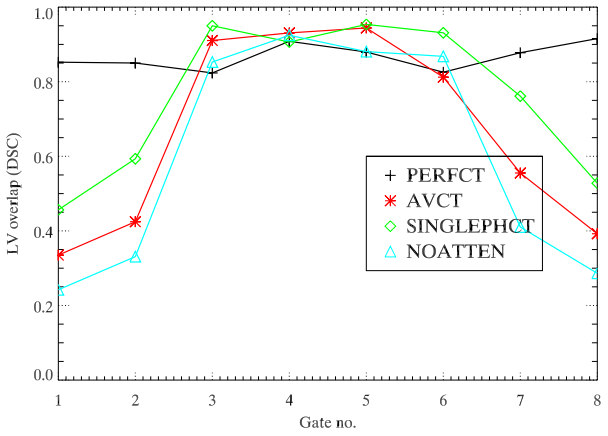

Fig. 3. **Full** images, shallow breathing, PET-to-HRCT registration. The HRCT was roto-translated with parms no.0 and smoothed. Different ACM procedures are compared.

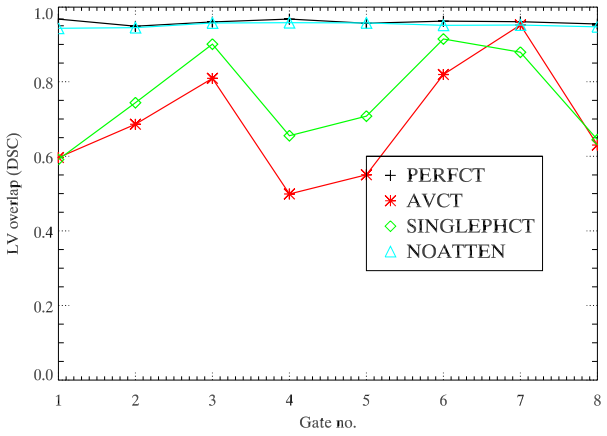

Fig. 4. **Cropped** images, shallow breathing, PET-to-HRCT registration. The HRCT was roto-translated with parms no.0 and smoothed. Different ACM procedures are compared.

III. Results and Discussion

A. Full vs. cropped images

As a first test, registration between *full* PET and CT images was attempted. The use of full images would be advantageous in that no preprocessing of the images (i.e. cropping) is needed. Regardless of the ACM used, however, registration of full images only yielded good results when similar respiratory phases needed to be matched (see Fig. 3). Additionally, it is very sensitive to the initial alignment between the two images (not shown).

For this reason, registration of the cropped images was tried. The cropping procedure requires an active participation of the user and takes a few seconds before the actual registration process can take place. However, the time lost is regained in computational speed (registration of cropped images is almost 10 times faster than registering the full-FOV images).

When cropping was applied, overall registration performances improved when compared to the ones obtained with full images.

In Fig. 4, two different behaviors can be discerned. PERFCT and NOATTEN datasets managed to achieve a nearly perfect alignment to the HRCT ($DSC \cong 1$). AVCT and SPHCT, on the other hand, performed well only in a few selected gates, namely the ones where the contribution of motion artefacts was least pronounced.

B. Effect of additional HRCT masking

As Fig. 5 shows, application of the additional HRCT masking was found to be beneficial for AVCT and SPHCT(compare to Fig. 4). Registration results between PERFCT datasets and HRCT were not affected by it. Except for a few isolated gates, NOATTEN datasets achieved good DSCs too.

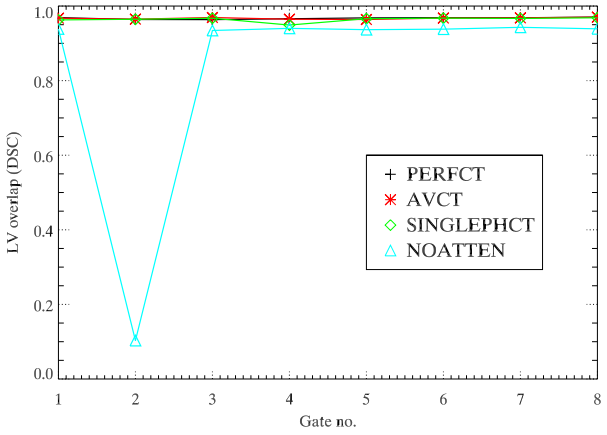

Fig. 5. Cropped images, shallow breathing, **PET-to-HRCT** registration. The HRCT was roto-translated with parms no.0, **masked** and smoothed. Different ACM procedures are compared.

Since this approach yielded better results, all the subsequent simulations were performed on cropped datasets and using the masked HRCT images.

C. Direct vs. indirect registration

A good initial alignment between the PET and the HRCT was found to be important, especially for registration of NOATTEN PET images (see blue curves on Fig. 5 and 6, results for different positions of the HRCT).

With this in mind, an intermediate PET-to-PET registration was performed, before starting the PET-to-HRCT registration. As illustrated in Fig. 6, the preliminary initial alignment of the

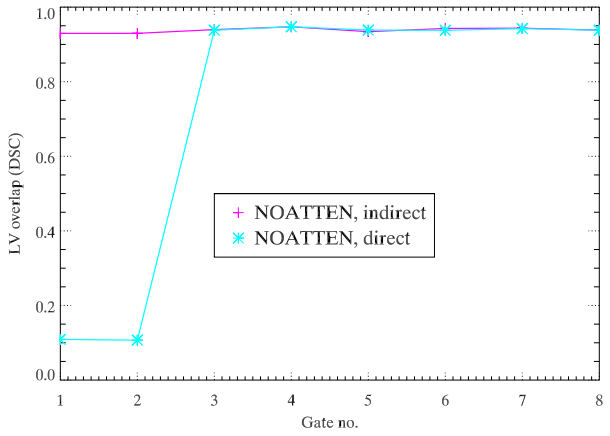

Fig. 6. Cropped images, shallow breathing. The HRCT was roto-translated with **parms no.18**, masked and smoothed. PET images were reconstructed without attenuation correction. **Indirect vs direct** PET-to-HRCT registration.

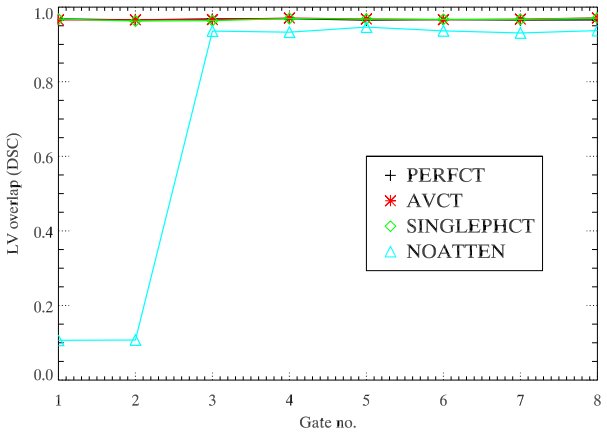

Fig. 7. Cropped images, shallow breathing, **HRCT-to-PET** registration. The HRCT was roto-translated with parms no. 0, masked and smoothed. Different ACM procedures are compared.

PET gates often affects DSCs positively. The curve plotting DICE coefficients for the 'indirectly registered' images shows improved overlap for the most distant frames. The frames closest to HRCT are not negatively influenced by the additional registration step.

D. PET-to-HRCT vs HRCT-to-PET

The results discussed so far were obtained by registering the PET (low resolution image, 2 mm voxel size) to the HRCT (high resolution image, 0.8 mm voxel size). Registration of the HRCT to the low-resolution PET has also been evaluated. Fig. 7 shows the results of the registrations between the same images as presented in Fig. 5, but with the registration direction inverted – i.e. HRCT-to-PET instead of PET-to-HRCT.

The results obtained were encouraging. PET-to-HRCT registration translates into a supersampling of PET to match the CT voxel size during every step of the registration process. This is more time consuming (about 3 times slower) and actually not necessary, as the subsequent PVC would be performed in PET space anyway. Fig. 7 shows that HRCT-to-PET registration is feasible for PERFCT, AVCT and SPHCT without any loss in registration quality.

E. Original vs smoothed HRCT

The results shown so far have been obtained with a smoothed HRCT. We found that matching PET and CT resolution is beneficial and useful to stabilize the registration results. This is particularly true for PET-to-HRCT registrations (see Fig. 8 in comparison to Fig. 5), whereas HRCT-to-PET registrations seem to be less sensitive to HRCT smoothing. The reason for this behaviour probably lies in a smoothing of HRCT details, which would otherwise introduce extra pixel clusters which may bias the registration results using NMI.

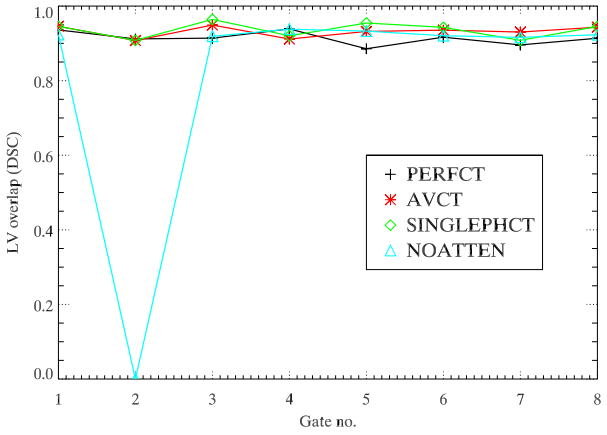

Fig. 8. Cropped images, shallow breathing, PET-to-HRCT registration. HRCT roto-translated with parms no.0 and **not smoothed**. Different ACM procedures are compared.

Downsampling the HRCT to the PET voxel size already implicitly smooths away extra details from the HRCT, such that the HRCT-to-PET relies less on the HRCT smoothing.

F. Deep breathing vs shallow breathing

A deep breathing scenario was also briefly analyzed (see Fig. 9), in order to be predictive for an extreme patient study. When deep breathing is considered, only for the PET dataset corrected with PERFCT acceptable results could be achieved for most gates. The artefacts introduced by the use of the other ACMs usually hampered the registration, regardless of the initial position of the HRCT.

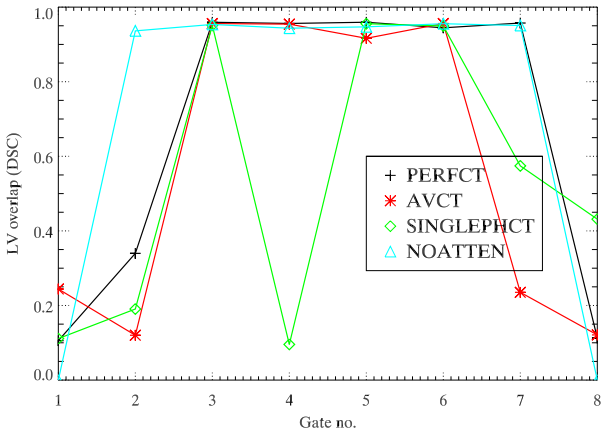

Fig. 9. Cropped images, PET-to-HRCT registration, **deep breathing**. HRCT is roto-translated with parms no. 0, masked and smoothed. Different ACM procedures are compared.

Results obtained when registering HRCT to NOATTEN datasets were comparable or superior to PERFCT with certain HRCT rotations (e.g. compare the blue and the black curve in Fig. 9). However, when other HRCT initial positions were considered, results were poor, confirming that registration of the NOATTEN PET images is sensitive to the initial alignment between PET and HRCT.

IV. Conclusions

Cropping images to the heart region was found to be beneficial to achieve acceptable LV alignment. This process requires little image preprocessing, but greatly enhances registration quality and computation times.

Average (AVCT) and single-phase (SPHCT) ACMs behave well in the case of shallow breathing, especially when an additional, simple masking is applied to HRCT images.

NOATT datasets tend to rely on a very good initial alignment between PET and HRCT, which can be obtained by means of a preliminary PET-to-PET registration. When this is achieved, they produced good results even in case of deep breathing. Hence, this preliminary PET-to-PET rough alignment is advisable to obtain acceptable registration results, especially when very different respiratory phases need to be matched or when the initial mismatch between PET and HRCT is significant.

The use of an attenuation map that perfectly matches its corresponding respiratory gate (PERFCT), though being the one often achieving the best registration results between any PET gate and a HRCT, is not realistically feasible. The results obtained with it need to be considered as the ideal results one should aim at.

HRCT-to-PET registration was found to be as effective as PET-to-HRCT registration. This is fortunate because HRCT-to-PET registration is faster and avoids unnecessary PET supersampling during registration. Moreover, HRCT-to-PET is less sensitive to HRCT variations (e.g. smoothing).

References

[1] M.J. Knuuti et al. "The value of quantitative analysis of glucose utilization in detection of myocardial viability by PET." *J Nucl Med* vol. 34, pp.2068-75, 1993.

[2] Nowak B et al. "Cardiac resynchronization therapy homogenizes myocardial glucose metabolism and perfusion in dilated cardiomyopathy and left bundle branch block." *J Am Coll Card*, vol. 41, pp.1523-8, 2003.

[3] M. Rajaram et al. "Cardiac PET/CT Misregistration Causes Significant Changes in Estimated Myocardial Blood Flow." *J Nucl Med*, vol. 54, pp.50-4, 2013.

[4] G. Porenta et al. "Parameter estimation of cardiac geometry by ECG-gated PET imaging: validation using magnetic resonance imaging and echocardiography." *J Nucl Med*, vol. 36, pp. 1123-9, 1995.

[5] G. J. Klein et al. "Real-time system for respiratory-cardiac gating in positron tomography." *IEEE Trans Nucl Sci*, vol. 45, pp.2139-2143, 1998.

[6] L. Ruthotto et al. "A Simplified Pipeline for Motion Correction in Dual Gated Cardiac PET." *BVM*,pp. 51-56, 2012.

[7] S.Y. Chun et al. "MRI-Based Nonrigid Motion Correction in Simultaneous PET/MRI." *J Nucl Med*, vol. 53, pp. 1284-1291, 2012.

[8] F. Büther et al. "List Mode-Driven Cardiac and Respiratory Gating in PET", *J Nucl Med*, vol. 50, pp.674:681, May 2009

[9] X. Ouyang et al. "Incorporation of correlated structural images in PET image reconstruction". *IEEE Trans. Med. Imag.*, vol. 13, no. 4, pp. 627-640, 1994.

[10] T. Sun, G. S. P. Mok, "Techniques for respiration-induced artifacts reductions in thoracic PET/CT".*Quant Imaging Med Surg*, vol. 2, pp. 46-52, 2012.

[11] M. J. Park et al. "Generation and evaluation of a simultaneous cardiac and respiratory gated Rb-82 PET simulation." *IEEE Nuclear Science Symposium Conference Record* 2011, pp.3327:3330.

[12] W. P. Segars et al. "4D XCAT phantom for multimodality imaging research." *Med Phys* , 37(9), 4902:15, 2010.

[13] R. Boellaard, "Standards for PET Image Acquisition and Quantitative Data Analysis.", *J. Nucl. Med.* vol. 50 (Suppl 1) pp. 11:20, 2009.

[14] E. O. Gerscovich et al. "Ultrasonographic Evaluation of Diaphragmatic Motion." *J Ultrasound Med* vol.20, pp.597:604, 2001.

[15] M. Ragnarsdottir, E K. Kristinsdottir. "Breathing movements and breathing patterns among healthy men and women 20-69 years of age. Reference values." *Respiration*. vol. 73(1), pp.48:54, 2006.

[16] M. Brambilla et al. "Performance Characteristics Obtained for a New 3-Dimensional Lutetium OxyorthosilicateBased Whole-Body PET/CT Scanner with the NEMA NU 2-2001 Standard." *J Nuc Med*, vol. 46(12), 2005.

[17] McLeish et al. "A study of the motion and deformation of the heart due to respiration." *IEEE transactions on medical imaging*, vol. 21(9), pp. 1142:50, 2002.

[18] C. Studholme et al. "An overlap invariant entropy measure of 3D medical image alignment.", *Pattern Recognition*, vol. 32, pp. 71:86, 1999.